



Design of a Biorthogonal Wavelet Transform Based R-Peak Detection and Data Compression Scheme for Implantable Cardiac Pacemaker Systems

Ashish Kumar¹ · Manjeet Kumar¹  · Rama Komaragiri¹

Received: 18 December 2017 / Accepted: 2 April 2018 / Published online: 19 April 2018
© Springer Science+Business Media, LLC, part of Springer Nature 2018

Abstract

Bradycardia can be modulated using the cardiac pacemaker, an implantable medical device which sets and balances the patient's cardiac health. The device has been widely used to detect and monitor the patient's heart rate. The data collected hence has the highest authenticity assurance and is convenient for further electric stimulation. In the pacemaker, ECG detector is one of the most important element. The device is available in its new digital form, which is more efficient and accurate in performance with the added advantage of economical power consumption platform. In this work, a joint algorithm based on biorthogonal wavelet transform and run-length encoding (RLE) is proposed for QRS complex detection of the ECG signal and compressing the detected ECG data. Biorthogonal wavelet transform of the input ECG signal is first calculated using a modified demand based filter bank architecture which consists of a series combination of three lowpass filters with a highpass filter. Lowpass and highpass filters are realized using a linear phase structure which reduces the hardware cost of the proposed design approximately by 50%. Then, the location of the R-peak is found by comparing the denoised ECG signal with the threshold value. The proposed R-peak detector achieves the highest sensitivity and positive predictivity of 99.75 and 99.98 respectively with the MIT-BIH arrhythmia database. Also, the proposed R-peak detector achieves a comparatively low data error rate (DER) of 0.002. The use of RLE for the compression of detected ECG data achieves a higher compression ratio (CR) of 17.1. To justify the effectiveness of the proposed algorithm, the results have been compared with the existing methods, like Huffman coding/simple predictor, Huffman coding/adaptive, and slope predictor/fixed length packaging.

Keywords Electrocardiogram (ECG) · Run-length encoding (RLE) · Lowpass and Highpass filter · Continuous wavelet transform (CWT) · Discrete wavelet transform (DWT) · Wavelet filter bank (WFB)

Introduction

Medical expenditures are on the all-time surge and high with the fast growth in world population. Healthcare became an

important agenda of both individuals and governments. The latest reports from World Health Organization purport that dealing with aging population is the important thing today [1]. The present healthcare structures and approaches are facing more significant challenges of dealing with the healthcare problems of aging population. Accordingly, spotting human diseases in a cost-effective, well timed and in a precise fashion has taken center stage [2–5]. Electrocardiogram (ECG) monitoring became ubiquitous because of its supremacy in the diagnosis of heart-related diseases and is also making its way both in hospitals and research areas [6].

The present medical fraternities are dependent on the usage of large conventional ECG equipment with multiple electrodes for ECG data acquisition. ECG equipment having twelve electrodes is the norm of the day and suffers from the capabilities of efficient data handling even on a short-term

This article is part of the Topical Collection on *Mobile & Wireless Health*

✉ Manjeet Kumar
manjeetchhillar@gmail.com

Ashish Kumar
akumar.1june@gmail.com

Rama Komaragiri
rama.komaragiri@bennett.edu.in

¹ Department of Electronics and Communication Engineering, Bennett University, Greater Noida, U.P 201308, India

basis. As the equipment has portability limitations, the activities of the patient are measured only during data collection, thus making continuous patient monitoring a tedious task. As ECG acquisition devices are not only costly but need training for home use, patients need to visit hospital frequently. The frequent visits to the hospital have severe limitations like irregular health monitoring, increase in hospital 's burden and causing physical hardship to the patients. Hence, the need of the day is a cheap, simple, portable, reliable and long-term ECG signal monitoring system [7].

Many long-term ECG signal monitoring approaches have been proposed during last few decades. First ECG signal monitoring system based on system-on-chip was introduced in [8], but this system consumes significant amounts of energy as it transmits raw data. Hence, a joint system for both ECG detection and data compression is highly required. An ECG monitoring system used in processing ECG signal for wireless transmission is shown in Fig. 1 [9].

The ECG monitoring system has three main functions namely, ECG signal analysis, data compression and wireless transmission. An ECG is a life-saving diagnostic tool in the heart care segment and is the most important feature amongst all ECG features is its QRS complex. A typical ECG signal is shown in Fig. 2. Hence, automatic detection of a QRS complex is the most important aspect of ECG signal processing and analysis. The performance of any ECG detection algorithm mainly relies on the QRS complex (R-peak) detector's accuracy [10, 11]. Many algorithms are presented in the literature to detect QRS complex. Some of the QRS complex detection algorithms, namely are time domain [12], ECG morphology [13], time-frequency domain (Wavelet) [14–19], and combined algorithms [20]. The wireless transmission of raw ECG data consumes high power, and use of local storage increases the device cost. So, data compression is required to reduce the power consumption and device cost.

Several lossy and lossless ECG data compression techniques have been reported in [21–24]. A comprehensive review of existing ECG signal denoising and R-peak detection is reported in [25]. Increasing detection accuracy with the help of complex signal processing techniques is the aim of most of the reported approaches. Low power consumption and less hardware complexity are the two crucial attributes of mobile ECG equipment. Low power implementation of many ECG detection and data compression techniques are reported in [21–25]. Until now, most of the existing work separately concentrates either on QRS complex detection or data compression techniques. There are few techniques which use a single algorithm to detect QRS complex as well compress ECG signal data [9, 26]. However, the techniques which use the same algorithm to detect QRS complex and compress ECG signal data possess high system complexity. Efforts are made to find an efficient algorithm which can be used to detect QRS complex and compress ECG signal data with low system complexity.

In this work, an algorithm based on bi-orthogonal wavelet transform is used to design the proposed QRS complex detection and to compress the ECG signal data. Here, run-length encoding technique is proposed for lossless data compression. The proposed design reduces the overall circuit complexity by reducing the number of delay elements, adders, and multiplexers. Sensitivity, positive predictivity, data error rate, compression ratio are the performance measures considered to evaluate the performance of the proposed design.

The remaining paper is organized as follows: Section II provides information about proposed design including wavelet selection, ECG signal denoising, ECG detection, ECG data compression and the complete architecture of the proposed method. The performance evaluation and the simulation results of the proposed technique are detailed in Section III. Finally, Section IV concludes the paper.

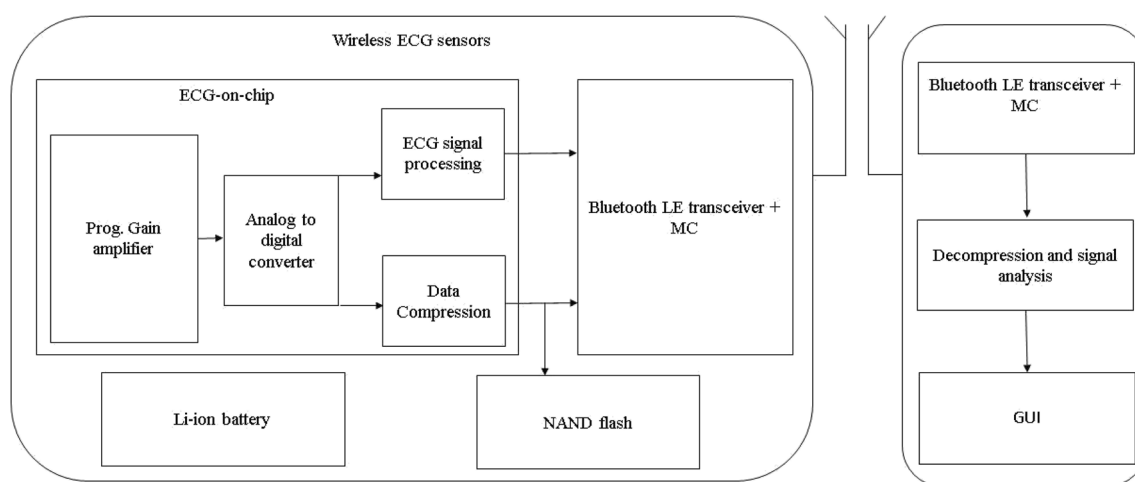
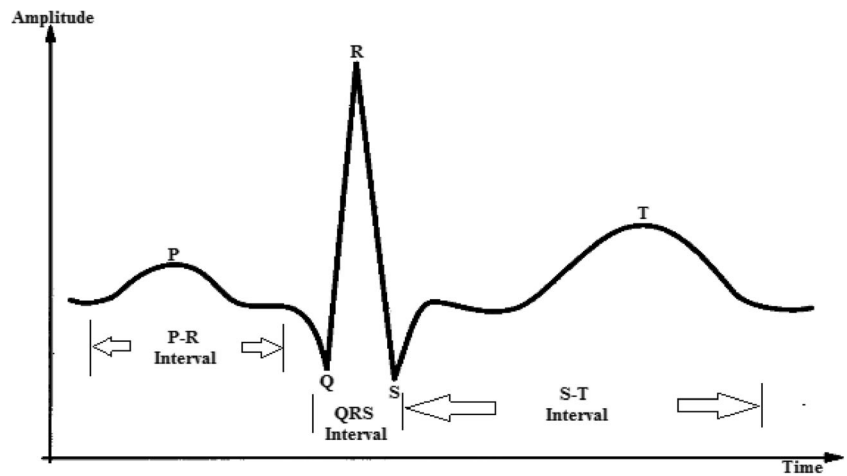


Fig. 1 Block diagram of ECG monitoring system [9]

Fig. 2 Typical ECG waveform of a single heartbeat



Proposed design

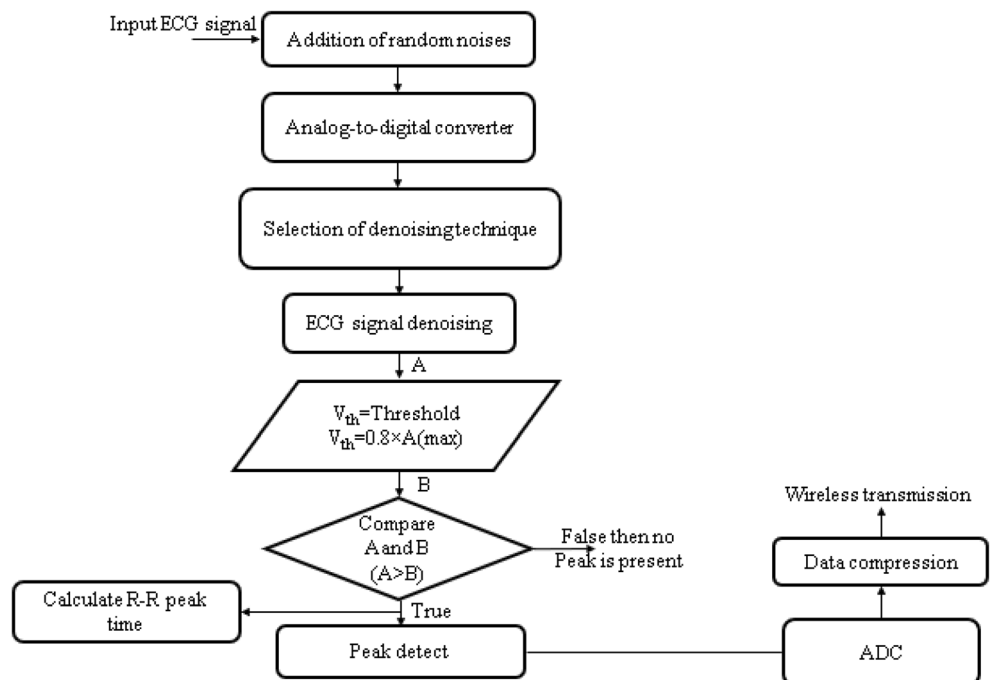
The methodology used to implement the proposed joint QRS complex detector and data compression design is presented in this section. Flowchart of the proposed R-peak detector with data compression technique is shown in Fig. 3.

Different steps shown in the flowchart are as follows. Input ECG signal is taken from Massachusetts Institute of Technology Boston’s Beth Israel Hospital (MIT-BIH) arrhythmia database [27] in .mat format. ECG signal from MIT-BIH may be or may not be corrupted with different noises, but in reality, ECG signals get corrupted due to the presence of various types of noises. In practice, Electrosurgical noise, muscle contraction, instrumentation noise, baseline drift, 60 Hz power line interference are different noise sources which corrupt the

ECG signal. A corrupted ECG signal is realized by adding random noise to ECG signal from MIT-BIH arrhythmia database. Adding random noise to the signal helps measure the efficiency of the proposed algorithm to reject noise from the signal. It is highly desirable to select a suitable denoising algorithm from the existing ECG signal denoising and QRS complex detection approaches available in the literature [25]. Reduced hardware complexity and a better detection accuracy make the wavelet transform based denoising, and QRS complex detection approaches as a most suitable technique when compared to the other techniques time domain, ECG morphology, and combined approaches [2].

The biorthogonal wavelet transform with four levels of decomposition is used to analyze a noisy ECG signal. The typical frequency range of an ECG signal is from 0.5 Hz to

Fig. 3 Flowchart of the proposed R-peak detector and data compression technique



150 Hz, and that of QRS complex is from 8 Hz to 20 Hz [28]. After the third level of decomposition, the frequency components that are left behind are in the 45 Hz range. The output of the third level wavelet filter bank is used as input to the fourth level wavelet filter bank whose output contains signals in the frequency range which matches with the frequency range of QRS complex. These signals from the fourth level wavelet filter bank are used for further processing as their frequency component matches with that of the QRS complex. After denoising, a QRS complex detector is designed in which incoming denoised ECG signal (A) is compared with a predetermined threshold value (V_{th}). The most critical criterion in fixing V_{th} value is that, neither an R-peak in the QRS complex is missed, nor a false R-peak is detected. The reasons for selecting a suitable value of V_{th} are as follows. If the value of V_{th} is very small, a lot of false R-peaks are detected thus reducing the detection accuracy and also the computational efforts are increased. A large value of V_{th} may fail to detect a true R-peak, thus affecting the detection accuracy. To minimize the computational efforts and to improve the detection accuracy, selection of V_{th} plays a very crucial role. An R-peak is only detected if the value of A is greater than the set threshold. After identifying the R-peaks, the time interval between two consecutive R-peaks is computed. The detected data is compressed using lossless data compression technique which is RLE in this case, further utilized for the wireless transmission for medical assistance.

Dataset

ECG signal from various databases like MIT-BIH arrhythmia database (MITDB), QT database (QTDB) [29] are used to evaluate the proposed design. MITDB contains 47 half-hour recordings of annotated ECG signals with a sampling frequency of 360 Hz and QTDB contains 105 records with a sampling frequency of 250 Hz.

Selection of wavelet transform and wavelet architecture

ECG signals exhibit slowly changing trends or oscillations punctuated with transients. To accurately analyze an ECG signal with abrupt changes, a new class of well-localized functions in time and frequency are needed. Wavelet transform which is a rapidly decaying wave-like oscillation that has zero mean and exists for a finite duration satisfies this condition. Continuous wavelet transform (CWT) and discrete wavelet transform (DWT) are thus useful to analyze ECG signals. DWT is ideally used to denoise and compresses signals and images and useful in representing many naturally occurring signals with fewer coefficients.

Accurate estimation of ECG signal parameters demands a suitable choice of basis function which is either symmetric or

antisymmetric [30]. Peak detection is facilitated by detecting extrema in case of symmetric basis and by identifying zero crossing in case of antisymmetric basis. By reducing the number of steps, a basis function with minimal sign changes simplifies the parameter estimation algorithm. As listed in Table 1, biorthogonal wavelet transform satisfies the abovementioned requirements, hence used in this work.

Due to low computational complexity, the biorthogonal wavelet transform is considered to implement QRS complex detectors [30]. Biorthogonal wavelet transform requires decimator and undecimator based architectures with lowpass and highpass filters as presented in [14, 31, 32].

In biorthogonal wavelet transform technique, ECG signal is first filtered using a combination of lowpass and highpass filters to yield lowpass and highpass sub-bands. As per Nyquist criterion, after filtering, half the samples are thrust aside. While realizing the filters, due to the smaller number of coefficients, these filters result in reduced computational complexity. These filters can also be used to reconstruct the sub-bands while canceling any aliasing which occurs due to downsampling. In the next level of decomposition, the sub-bands are iteratively filtered by the technique above (combination of lowpass and highpass filters) to yield narrow sub-bands. However, the cascading of filters increases hardware complexity and power consumption in the circuit [33]. In this work, to reduce the hardware complexity and power consumption, a new demand-based wavelet filter bank architecture is proposed. Figure 4 shows the proposed wavelet filter bank architecture. In the proposed demand based wavelet filter bank architecture, ECG signal is first passed through a cascade connection of three lowpass filters and then through a highpass filter.

The proposed architecture only requires three lowpass filters, and a highpass filter when compared to the filter bank architectures used in [14]. Also, hardware cost, as well as power consumption of the proposed design, can be further reduced by realizing the filters using FIR types. The transfer function of lowpass and highpass filters are obtained as shown in Eq. (1) and Eq. (2)

$$H(z) = 0.125 + 0.375z^{-1} + 0.375z^{-2} + 0.125z^{-3} \quad (1)$$

$$G(z) = -2 + 2z^{-1} \quad (2)$$

Comparison of proposed demand-based wavelet filter bank architecture with [14] is discussed in Table 2.

A multiplier is a circuit element that requires more area and power as a minimum of the four adders are required to implement a multiplier. As listed in Table 2, the proposed work needs only seven multipliers against thirteen in [14] and twenty-six in [24]. In addition, the proposed work requires only four adders as compared to sixteen in [14] and thirty-two in [31].

Table 1 Properties of different wavelet transforms

Wavelet type	Compact support	Key properties	Implementation
Orthogonal splines	No	Symmetry and regularity + orthogonality	IIR/FIR
Semi-orthogonal splines	Analysis or synthesis	Symmetry and regularity + optimal time-frequency localization	Recursive IIR/FIR
Shift-orthogonal splines	No	Symmetry and regularity + Quasi-orthogonality +fast decaying wavelet	IIR
Biorthogonal Splines	Yes	Symmetry and regularity + compact support	FIR

Hardware comparison in terms of area and power of the proposed wavelet filter bank with the existing methods are listed in Table 3. It is observed from Table 2 that the proposed wavelet filter bank architecture requires four adders, seven multipliers, and ten delay elements. Thus, the area needed to realize these adders and multipliers are $1160 \mu\text{m}^2$ and $15,109.92 \mu\text{m}^2$, respectively, which is comparatively lower than the existing reported methods [14, 31]. In the proposed wavelet filter bank architecture, the power consumed by adders and multipliers is $408 \mu\text{W}$ and $3047.17 \mu\text{W}$, respectively, which is comparatively lower than the existing reported methods [14, 31]. A complete

comparison between the proposed architecture and existing architectures is presented in Table 3.

QRS complex detection

The incoming peaks are compared with a threshold value. The threshold value is determined after passing the ECG signal through wavelet filter bank. Two types of threshold values namely hard threshold and soft threshold can be used to compare the peak. The peaks which are having a peak value less than the threshold are viewed to be zero in

Fig. 4 (a) Recursive application of wavelet filter bank. (b) Wavelet filter bank. (c) Schematic of the lowpass filter in wavelet filter bank. (d) Schematic of a highpass filter in wavelet filter bank

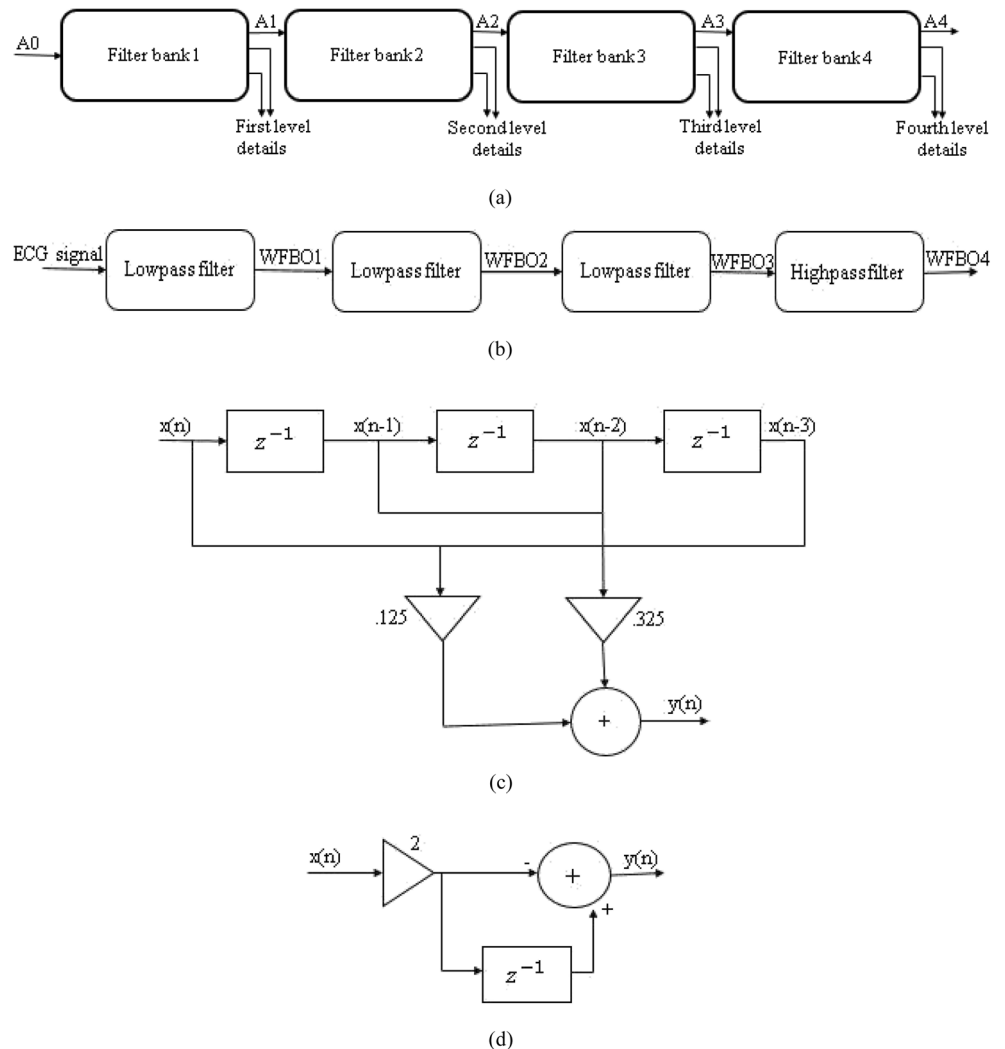


Table 2 Comparison of proposed architecture with existing methods

Design Technique	Proposed	[14]	[31]
Lowpass filters	3	3	3
Highpass filters	1	4	4
Delay elements	10	13	NR
Adders	4	16	32
Multipliers	7	13	26

both hard and soft thresholds. Thus, the functionality of both hard and soft threshold values is same in the case of those peaks with peak value less than the set threshold. For the peaks with a peak value larger than a set threshold, both hard threshold, and the soft threshold result in different functionality. In case of the hard threshold, those peaks having a value larger than the set threshold are forced to approach towards one thus detecting the presence of a peak. In doing so, some features of the signal are lost and hence using hard threshold degrades the computational accuracy. In the soft threshold, the value of the peaks is retained if the value of the peak is larger than the threshold value. Hence, for the proposed QRS detector, using soft threshold is more advantageous than using the hard threshold. Eq. (3) defines the threshold value used in this work.

$$V_{th} = 0.8 \times A(\max) \quad (3)$$

A peak having a value larger than the defined threshold value is considered to be an R-peak. Thus, by identifying the R-peaks, the time interval between two consecutive R-peaks is calculated.

The reason for selecting the above-said threshold values is as follows. Different values of the threshold are used to detect R peak. The threshold value neither should result in false peak detection nor should miss a peak. Further, setting a large value of threshold results in missed peaks thus increasing the detection error rate. Whereas, setting a small value of threshold results in increased computation complexity and false detection thus reducing the detection efficiency of the system. Different

values of V_{th} ranging from 0.7 to 0.9 are considered. V_{th} close to 0.7 resulted in an increased false peak detection, whereas, V_{th} close to 0.9 resulted in R-peaks being discarded. Hence the threshold value is chosen to be $0.8 \times A(\text{maximum})$. Threshold values other than the proposed either detect an extra number of ECG peaks or detects less number of ECG peaks.

Data compression

Lossy and lossless are two types of compression techniques. Compression ratio (CR) of lossy compression techniques is high, but medical regulatory bodies do not approve these techniques in many countries [9], thus prohibiting the commercial use of lossy compression techniques is prohibited. In the lossless technique, as there is no chance of losing any information about potential diagnostic value, the lossless technique is the only option available and used in the proposed work. Many lossless ECG compression techniques presented in the literature [21–24] have focused on achieving high compression ratio. Here in the proposed work, various data compression techniques namely wavelet transform, Huffman coding/simple predictor, Huffman coding/adaptive, slope predictor/fixed length packaging and run-length encoding are tested, but run-length encoding is chosen based on its high compression ratio. In this method, the detected R-peaks are represented by “1” and “0” represents the rest of the data. This data is then compressed by replacing the zeros between two peaks by the number of zeros between the peaks. Run-length encoding (RLE) is a well-known, simple, and quick form of lossless data compression technique which offers a significant amount of compression for a specific type of data stream (in which the same data value occurs in many consecutive data elements). The run-length encoding decreases the size of a given signal, while at the same time not losing any information from the original. Each packet of Run-length encoding consists of two components, namely, *run_count* which denotes the number of characters in the run, and *run_value* which indicates the common value of the characters in the run. For example, using RLE, the string of datas *111,111,111,111,000,011,111,110,000,001,100* encoded after string compression results in *1,214,071,602,120*. This can be interpreted as a sequence of twelve *1* s, four *0* s, seven

Table 3 Area and power comparison of adders and multipliers of proposed wavelet filter bank with existing ones

Method	Number of Adders	Area Required for Adders (290 μm^2 per adder [34])	Power Required for Adders (102 μW per adder [34])	Number of Multipliers	Area Required for Multipliers (2158.56 μm^2 per Multiplier [35])	Power Required for Multipliers (435.31 μW per adder [35])
[14]	16	4640 μm^2	1632 μW	13	28,061.28 μm^2	5659.03 μW
[31]	32	9280 μm^2	3264 μW	26	56,122.56 μm^2	11,318.03 μW
Proposed	4	1160 μm^2	408 μW	7	15,109.92 μm^2	3047.17 μW

1 s, six 0 s, two 1 s and two 0 s. After that, RLE is applied to the binary matrix. Compression ratio is calculated using Eq. (4).

$$CR = \frac{N_0}{N_1} \tag{4}$$

where, N_0 = the number of uncompressed samples \times bit width of uncompressed samples and N_1 = the number of compressed samples \times bit width of compressed samples.

Architecture

The block diagram of the complete architecture of proposed design is shown in Fig. 5. The proposed design mainly consists of three blocks. Namely, demand-based wavelet filter bank architecture with a linear phase structure realization for ECG signal denoising, modified soft threshold based QRS complex detector to detect R-peak, and data compression to compress the detected ECG data which is also used for the wireless transmission for medical assistance. In the existing wavelet filter banks, Mallet based wavelet filter bank architecture is used in which signal is decomposed into two parts namely into approximation and detail. Since all the peaks of ECG signal present in the frequency range of 10 to 100 Hz, a demand-based wavelet filter bank architecture with linear phase structure realization is proposed in the present work. The proposed wavelet filter bank consists of three lowpass filters namely FB1, FB2, FB3, and a highpass filter FB4.

It is found that the output of wavelet filter bank at fourth level is smooth and less noisy compared to other levels. Hence, fourth level wavelet filter bank is used for the proposed design. After that soft threshold with value $0.8 \times (max)A$ is chosen, which compares the output of wavelet filter bank four with the set threshold value and detects the peaks. After that, all detected peaks are considered as ‘1’ and undetected peaks are considered as ‘0,’ and a binary matrix is formed. Finally, data is compressed using RLE.

Performance results

The proposed work achieves an improved peak detection and higher data compression rate. These results were discussed in the following subsections.

QRS complex detection

ECG signal from various datasets namely MIT-BIH arrhythmia database (MITDB) and QTDB [30] are used to evaluate the proposed design. MIT-BIH arrhythmia database contains forty-seven half-hours recording of annotated ECG signals with a sampling frequency of 360 Hz. Whereas, the QT database contains 105 records with a sampling frequency of 250 Hz.

The proposed technique is tested with three different types of MIT-BIH arrhythmia database signals and QT database, namely short time data (10s. data from MIT-BIH and QT database), medium data (one-minute data from MIT-BIH and QT database) and full-length data (1-h data from MIT-BIH and QT database).

Further, false negative (FN) and false positive (FP) detections are used to evaluate the detection performance. FP is the number of extra detected peaks and FN is the number of missed peaks. Further, FN and FP are used to compute the sensitivity (Se %), positive predictivity (+P %), data error rate (DER %), the probability of missed detection (PD), and the probability of false alarms (PFA). Se%, +P%, DER, and PD are defined using Eq. (5) through Eq.

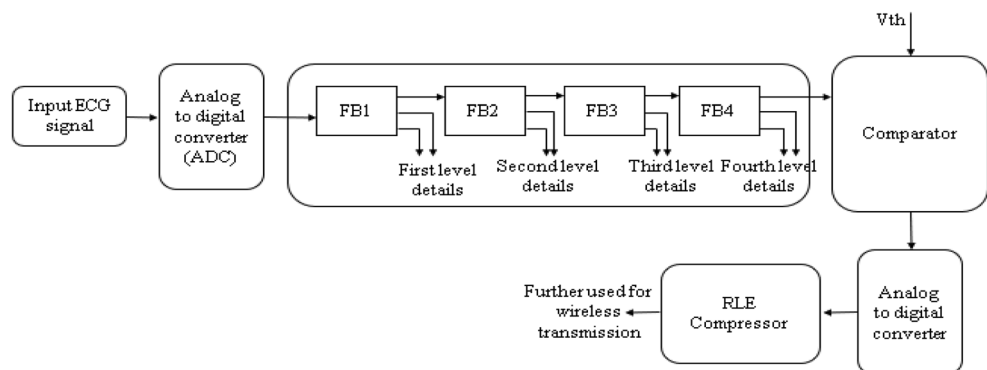
$$Se(\%) = \frac{TP}{TP + FN} \times 100 \tag{5}$$

$$+P(\%) = \frac{TP}{TP + FP} \times 100 \tag{6}$$

$$DER = \frac{FP + FN}{Total\ number\ of\ QRS\ peaks} \tag{7}$$

$$PD = 1 - \frac{TP}{TP + FN} \tag{8}$$

Fig. 5 Block diagram of proposed joint ECG detection and data compression scheme



where true positive (TP) is the number of correctly detected R-peaks. R-peak detection results for all records and different size of data, namely ten seconds, one minute, and full-length ECG data of MIT-BIH arrhythmia database are shown in Tables 4, 5 and 6, respectively. Table 5 shows the results of 10 s ECG data; Table 5 shows results of 1-min ECG data and Table 6 shows the results of 1-h ECG data.

As shown in Table 4, the proposed QRS complex detector achieves the highest sensitivity and positive predictivity of

99.31% and 99.65% with the MIT-BIH arrhythmia database of ten seconds. *108.mat* and *214.mat* signals from the MIT-BIH arrhythmia database contain maximum noise [25]. The proposed R-peak detector achieves the highest sensitivity and positive predictivity of 90.90% and 100% on *108.mat* and 100% sensitivity and positive predictivity on *214.mat*.

From Table 5, the proposed R-peak detector achieves the highest sensitivity and positive predictivity of 99.65% and 99.65% with the MIT-BIH arrhythmia database of one minute.

Table 4 Performance of the proposed technique using 10 Second MIT-BIH Database

Record No.	Total (beats)	True positive (TP)	False Negative (FN)	False positive (FP)	Failed detection (FN + FP)	Failed detection (%) (FN + FP) × 100/total	Se (%)	+P (%)	DER (10 ³)
100	13	13	0	0	0	0	100	100	0
101	11	11	0	0	0	0	100	100	0
102	12	12	0	0	0	0	100	100	0
103	11	11	0	0	0	0	100	100	0
104	13	13	0	0	0	0	100	100	0
105	14	14	0	0	0	0	100	100	0
106	10	10	0	0	0	0	100	100	0
107	12	11	1	0	1	8.33	91.66	100	0.83
108	11	10	1	0	1	9.09	90.90	100	.09
109	16	16	0	1	1	6.25	100	94.11	.06
111	12	12	0	0	0	0	100	100	0
112	14	14	0	0	0	0	100	100	0
113	09	09	0	0	0	0	100	100	0
114	10	10	0	0	0	0	100	100	0
115	10	10	0	0	0	0	100	100	0
116	14	14	0	0	0	0	100	100	0
117	9	9	0	0	0	0	100	100	0
118	12	12	0	0	0	0	100	100	0
119	10	10	0	0	0	0	100	100	0
121	10	10	0	0	0	0	100	100	0
122	15	15	0	0	0	0	100	100	0
123	9	8	1	0	1	11.11	90	100	.11
124	8	8	0	0	0	0	100	100	0
200	15	15	0	0	0	0	100	100	0
201	14	14	0	0	0	0	100	100	0
202	7	7	0	0	0	0	100	100	0
205	15	15	0	0	0	0	100	100	0
207	10	10	0	0	0	0	100	100	0
208	13	12	1	0	1	7.69	92.30	100	.076
209	15	15	0	0	0	0	100	100	0
210	16	16	0	0	0	0	100	100	0
212	15	15	0	0	0	0	100	100	0
213	18	18	0	0	0	0	100	100	0
214	13	13	0	0	0	0	100	100	0
215	18	18	0	0	0	0	100	100	0
217	12	12	0	0	0	0	100	100	0
219	13	13	0	0	0	0	100	100	0
220	12	12	0	0	0	0	100	100	0
221	13	13	0	0	0	0	100	100	0
222	13	13	0	0	0	0	100	100	0
223	13	13	0	0	0	0	100	100	0
228	12	12	0	0	0	0	100	100	0
230	14	14	0	0	0	0	100	100	0
231	10	10	0	0	0	0	100	100	0
232	9	9	0	1	1	.11	100	90	.11
233	17	17	0	0	0	0	100	100	0
234	15	15	0	0	0	0	100	100	0
Total	587	583	4	2	6	1.02	99.31	99.65	1.02

Table 5 Performance of the proposed technique using 1-Minute MIT-BIH database

Record No.	Total (beats)	True positive (TP)	False negative (FN)	False positive (FP)	Failed detection (FN + FP)	Failed detection (%) (FN + FP) × 100/total	Se (%)	+P (%)	DER (10 ³)
100	74	74	0	0	0	0	100	100	0
101	70	70	0	1	1	1.42	100	98.59	.014
102	73	73	0	0	0	0	100	100	0
103	70	70	0	0	0	0	100	100	0
104	74	73	1	0	1	1.35	98.64	100	.013
105	83	83	0	0	0	0	100	100	0
106	69	67	2	0	2	2.89	97.10	100	.028
107	71	71	0	0	0	0	100	100	0
108	58	58	0	0	0	0	100	100	0
109	91	91	0	0	0	0	100	100	0
111	69	69	0	0	0	0	100	100	0
112	85	85	0	0	0	0	100	100	0
113	58	58	0	0	0	0	100	100	0
114	55	55	0	0	0	0	100	100	0
115	63	63	0	0	0	0	100	100	0
116	79	79	0	0	0	0	100	100	0
117	50	50	0	0	0	0	100	100	0
118	73	73	0	0	0	0	100	100	0
119	65	65	0	0	0	0	100	100	0
121	60	59	1	0	1	1.66	98.33	100	.016
122	87	87	0	0	0	0	100	100	0
123	49	48	1	0	1	2.04	97.95	100	.020
124	50	50	0	0	0	0	100	100	0
202	53	53	0	0	0	0	100	100	0
205	89	89	0	0	0	0	100	100	0
209	92	92	0	0	0	0	100	100	0
210	91	89	2	0	2	2.19	97.80	100	.021
212	90	90	0	0	0	0	100	100	0
213	111	111	0	0	0	0	100	100	0
214	76	76	0	0	0	0	100	100	0
215	106	106	1	4	5	4.71	99.06	96.36	.047
217	72	72	0	0	0	0	100	100	0
219	74	74	0	0	0	0	100	100	0
220	72	72	0	0	0	0	100	100	0
221	79	78	1	0	1	1.26	98.73	100	.012
222	75	75	0	0	0	0	100	100	0
223	80	80	0	0	0	0	100	100	0
228	71	69	2	3	5	7.04	97.18	95.83	.070
230	79	79	0	0	0	0	100	100	0
231	63	63	0	0	0	0	100	100	0
233	103	103	0	0	0	0	100	100	0
234	92	92	0	0	0	0	100	100	0
Total	3144	3140	11	11	22	.699	99.65	99.65	.006

Table 6 Performance of the proposed technique using 1-h MIT-BIH database

Record No.	Total beats	True positive (TP)	False negative (FN)	False positive (FP)	Se (%)	+P (%)	DER (10 ³)	Accuracy
100	2273	2273	0	0	100	100	0	100
102	2191	2187	4	0	99.8174	100	0.1826	99.99
103	2090	2083	7	0	99.665	100	0.3349	99.99
107	2139	2136	3	0	99.8597	100	0.1403	99.99
113	1795	1795	0	0	100	100	0	100
117	1538	1533	5	3	99.6749	99.8047	0.5202	99.99
122	2478	2476	2	0	99.9193	100	0.0807	99.99
123	1518	1518	0	0	100	100	0	100
220	2068	2048	20	0	99.0329	100	0.9671	99.99
234	2763	2752	11	0	99.6019	100	0.3951	99.99
Total	20,853	20,801	52	3	99.75	99.98	.26	99.93

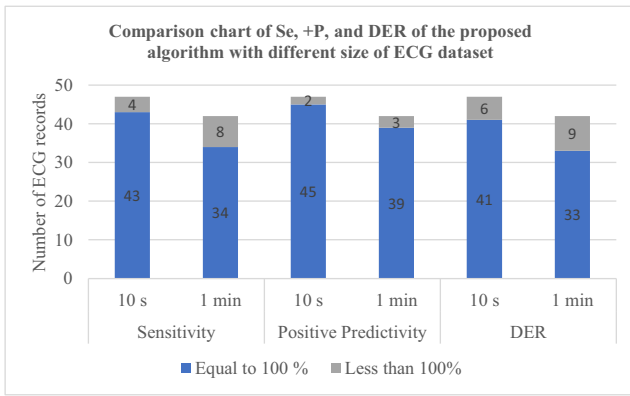


Fig. 6 Comparison chart of Se, +P, and DER of the proposed algorithm with different size of ECG dataset

Also, the proposed R-peak detector achieves the highest sensitivity and positive predictivity of 100% on *108.mat* and 100% sensitivity and positive predictivity on *214.mat* to existing detection algorithms.

Comparison chart of Se, +P, and DER of the proposed algorithm with different size of ECG dataset is shown in Fig. 6.

From Table 6, the proposed R-peak detector achieves the highest sensitivity and positive predictivity of 99.75% and 99.98% with the MIT-BIH arrhythmia database of full-length.

The performance of the proposed QRS complex detector under noisy conditions is shown in Fig. 7.

Figure 7(a) pictorially represents the *108.mat* input ECG signal taken from MIT-BIH arrhythmia database. To evaluate the proposed QRS detection algorithm, a random noise source as shown in Fig. 7(b) is generated and added to ECG signal in Fig 6(c). Figure 7(c) shows a noisy input ECG signal. The noisy input ECG signal is first filtered using a wavelet transform based lowpass filter, wavelet filter bank 1 (WFB1). The output of the WFB1 is shown in Fig. 7(d). The output of the WFB1 is further filtered using a wavelet transform based lowpass filter also known as wavelet filter bank 2 (WFB2). The output of WFB2 is shown in Fig. 7(e). The output of WFB2 is then filtered using a wavelet transform based lowpass filter known as wavelet filter bank 3 (WFB3). The output of WFB3 is shown in Fig. 7(f). The output of WFB3 is finally filtered using a wavelet transform based highpass filter known as wavelet filter bank 4 (WFB4). The output of WFB4 is shown in Fig. 7(g). Figure 7(h) shows the detected R-peaks. Figure 7(h) shows the 10 R-peaks in ten seconds of ECG data. Table 4 also shows the same number of R-peaks for the *108.mat* ECG data.

Performance comparison of existing techniques with the proposed technique is shown in Table 7.

Fig. 7 a 108 series of input ECG signal taken from MIT-BIH arrhythmia database, (b) randomly generated noise signal, (c) ECG signal contains noise, (d) wavelet filter bank-1 output, (e) Wavelet filter bank-2 output, (f) Wavelet filter bank-3 output, (g) Wavelet filter bank-4 output and (h) final output.

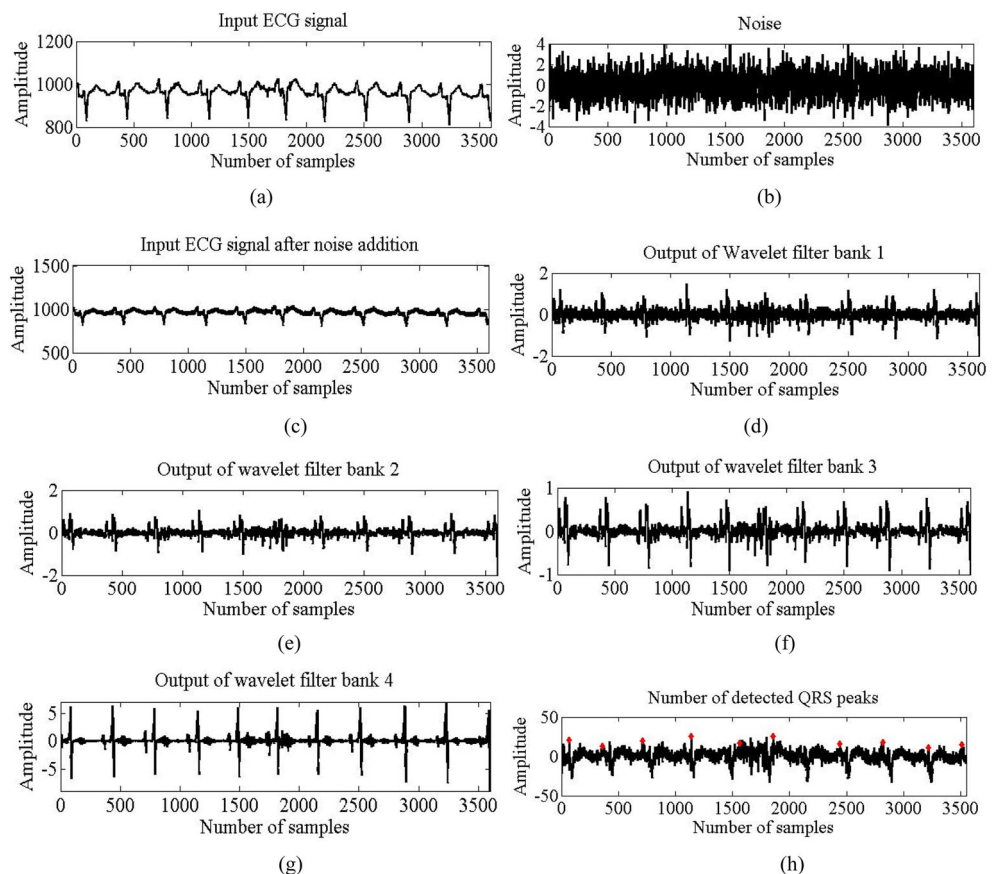


Table 7 Performance comparison of proposed technique with existing techniques

Method	Se (%)	+P (%)	Reference
Proposed	99.75	99.98	–
Real-time	97.63	97.33	[26]
Mathematical morphology	97.80	97.80	[36]
Wavelet denoising	99.50	99.49	[37]
Quadratic spline wavelet	99.31	99.70	[38]
Filter banks	99.59	99.56	[39]
Genetic algorithm	99.60	99.51	[40]

As shown in Table 7, the proposed technique has a better detection performance compared to existing techniques. Some methods like a genetic algorithm, filter bank also offer good performance, but their computational complexities are relatively high compared to proposed technique. The proposed technique requires less hardware when compared to the existing techniques like [14, 31] because of the use of modified demand based wavelet filter bank architecture, and linear phase structure realization. Hence, the proposed technique is better for both implantable as well as wearable cardiac pacemaker applications.

Data compression

The proposed ECG data compression technique is tested using QT database and MIT-BIH arrhythmia database. The bit compression ratio (BCR) is calculated using the formula in Eq. (9):

$$BCR = \frac{BW_{uncomp}}{BW_{comp}} \tag{9}$$

Here, BW_{uncomp} is the bit width of the uncompressed sample and BW_{comp} is the bit width of the compressed sample. The

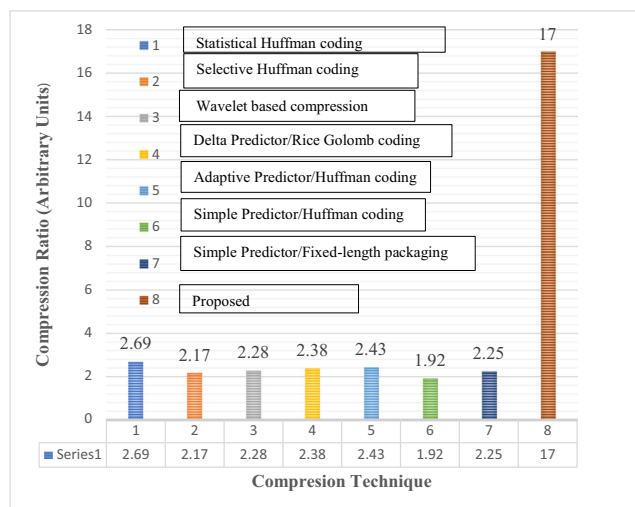


Fig. 8 Comparison of proposed technique with existing techniques

proposed ECG data compression technique gains a high compression ratio of 17.1. The other existing data compression techniques have very less compression ratio which is 2.66 for statistical Huffman coding, 2.17 for selective Huffman coding and 2.28 for wavelet-based data compression technique. Comparison of proposed technique with existing techniques is shown in Fig. 8.

Conclusion

In this work, a novel technique based on a biorthogonal wavelet transform that is jointly used for QRS complex detection and lossless ECG data compression aimed at implantable and wearable ECG devices is proposed. The R-peak detector achieves a high sensitivity of 99.75% and a positive predictivity of 99.98% with the MIT-BIH arrhythmia database and a sensitivity of 99.67% and positive predictivity of 99.9% with the QT database. The RLE -based ECG data compression technique provides a lossless compression ratio of 17.1The proposed technique requires approximately 50% less hardware compared to the existing techniques. The proposed methodology can be further extended to analyze other bio-medical signals.

Compliance with ethical standards

Conflict of interest Author Ashish Kumar declares that he has no conflict of interest. Author Manjeet Kumar declares that he has no conflict of interest. Author Rama Komaragiri declares that he has no conflict of interest.

Ethical approval This article does not contain any studies with human participants or animals performed by any of the authors.

References

1. Aging, In World Health Organization. <http://www.who.int/topics/ageing/en/>, 2016.
2. Banerjee, A., and Gupta, S., Analysis of smart mobile applications for healthcare under dynamic context changes. *IEEE Trans. Mob. Comput.* 14(5):904–919, 2015.
3. Zhang, Y., and et al., Health-CPS: Healthcare cyber-physical system assisted by cloud and big data. Accepted by IEEE Systems Journal.
4. Zhang, Y., Chen, M., Huang, D. et al., iDoctor: Personalized and professionalized medical recommendations based on hybrid matrix factorization. *Fut. Gener. Comput. Syst* 66:30–35, 2017.
5. Yang, Z., Zhou, Q., Lei, L., Zheng, K., and Xiang, W., An IoT-cloud based wearable ECG monitoring system for smart healthcare. *J. Med. Syst.*, 1–11, 2016.
6. Zou, Y., Han, J., Xuang, S., Huang, S., Weng, X., Fang, D., and Zeng, X., An energy-efficient design for ECG recording and R-peak detection based on wavelet transform. *IEEE Trans. Circ. Syst. -II Exp. Briefs* 62(2):119–124, 2015.

7. Liu, X., Zheng, Y., Phyu, M. W., Zhao, B., Je, M., and Yuan, X., Multiple functional ECG signals is processing for wearable applications of long-term cardiac monitoring. *IEEE Trans. Biomed. Eng.* 58(2):380–389, 2011.
8. Buxi, D., et al., Wireless 3-lead ECG system with on-board digital signal processing for ambulatory monitoring, in Proc. IEEE bio CAS, 308–31, 2012.
9. Deepu, C., and Lian, Y., A joint QRS detection and data compression scheme for wearable sensors. *IEEE Trans. Biomed. Eng.* 62(1): 165–175, 2015.
10. Merah, M., Abdelmalik, T. A., Larbi, B. H., R-peak detection based on stationary wavelet transform, *Comput. Meth. Prog. Biomed.*, 1–12, 2015.
11. Kumar, A., Komaragiri, R., and Kumar, M., From pacemaker to wearable: Techniques for ECG detection systems. *Journal of Medical Systems* 42(2):34, 2018.
12. Pan, J., and Tompkins, W. J., A real-time QRS detection algorithm. *IEEE Trans. Biomed. Eng.* 32(3):230–236, 1985.
13. Hu, Y. H., Tompkins, W. J., Urrusti, J. L., and Afonso, V. X., Applications of artificial neural networks for ECG signal detection and classification. *J. Electrocardiol.* 26:66–73, 1994.
14. Min, Y. J., Kim, H. K., Kang, Y. R., Kim, G. S., Park, J., and Kim, S. W., Design of Wavelet-Based ECG detector for implantable cardiac pacemakers. *IEEE Trans. on Biomedical Circuits and Systems* 7(4):426–436, 2013.
15. Bhavtosh, D. B. and Kumar, Y., High performance QRS complex detector for wearable ECG system using multi scaled product with booth multiplier and soft threshold algorithm, IEEE ICSC-15, 204–209, 2015.
16. Kumar, A., Berwal, D., Kumar, Y., Design of high-performance ECG detector for implantable cardiac pacemaker systems using biorthogonal wavelet transform (DOI: 10.1007/s00034-018-0754-3), 2018.
17. Abibullaev, B., and Seo, H. D., A new QRS detection method using wavelets and artificial neural networks. *Journal of medical systems* 35(4):683–691, 2011.
18. Sumathi, S., Beulah, H. L., and Vanithamani, R., A wavelet transform based feature extraction and classification of cardiac disorder. *Journal of medical systems* 38(9):98, 2014.
19. Benali, R., Reguig, F. B., and Slimane, Z. H., Automatic classification of heartbeats using wavelet neural network. *Journal of medical systems* 36(2):883–892, 2012.
20. S. M. Szilagyi and L. Szilagyi, Wavelet transform and neural-network-based adaptive filtering for QRS detection, in Proc. 22nd Annu. Int. Conf. IEEE Engineering in Medicine and Biology Soc., Chicago, 2:1267–1270, 2003.
21. Amavut, Z., ECG signal compression based on burrows-wheeler transformation and inversion ranks of linear prediction. *IEEE Trans. Biomed. Eng.* 54(3):410–418, 2007.
22. Miaou, S.-G., and Chao, S.-N., Wavelet-based lossy-to-lossless ECG compression in a unified vector quantization framework. *IEEE Trans. Biomed. Eng.* 52(3):539–543, 2005.
23. Chua, E., and Fang, W., Mixed bio-signal lossless data compressor for portable brain-heartmonitoring systems. *IEEE Trans. Consum. Electron.* 57(1):267–273, 2011.
24. Chen, S.-L., and Wang, J.-G., VLSI implementation of low-power costefficient lossless ECG encoder design for wireless healthcare monitoring application. *Electron. Lett.* 49(2):91–93, 2013.
25. Kohler, B.-U., Hennig, C., and Orglmeister, R., The principles of software QRS detection. *IEEE Eng. Med. Biol. Mag.* 21(1): 42–57, 2002.
26. Zhang, X., and Lian, Y., A 300-mV 220-nW event-driven ADC with real-time QRS detection forWearable ECG sensors. *IEEE Trans. Biomed. Circ. Syst.* 8(6):834–843, 2014.
27. Mark, R., Moody, G., MIT-BIH arrhythmia database. Available from: <http://www.physionet.org/physiobank/database/mitdb/>.
28. Elgendi, M., Jonkman, M., DeBoer, F., Frequency bands effects on QRS detection. *Pan*, 5, 15Hz, 2010.
29. Laguna, P., Mark, R. G., Goldberg, A., and Moody, G. B., A database for evaluation of algorithms for measurement of QT and other waveform intervals in the ECG. *Comput. Cardiol.*:673–676, 1997.
30. Sivannarayana, N., and Reddy, D. C., Biorthogonal wavelet transforms for ECG parameters estimation. *Med. Engg. Phy.* 21(3):167–174, 1999.
31. Rodrigues, J. N., Olsson, T., Sornmo, L., and Owall, V., Digital implementation of a wavelet-based event detector for cardiac pacemakers. *IEEE Trans. Circuits Syst. I, Reg. Papers* 52(12):2686–2698, 2005.
32. Mallat, S. G., A theory for multiresolution signal decomposition: The wavelet representation. *IEEE Trans. Pattern Anal. Mach. Intell.* 11(7):674–693, 1989.
33. Kumar, A., Tiwari, R. N., Kumar, M., Kumar, Y., A filter bank architecture based on wavelet transform for ECG signal denoising. In Signal Processing, Computing and Control (ISPCC), 2017 4th International Conference on (pp. 212–215). IEEE, 2017.
34. Levi, I., ALbeck, A., Fish, A., and Wimer, S., A low energy and high performance DM² adder, *IEEE Trans. Circ. & Circ. I: REGULAR PAPERS*, 61(11), 2014.
35. Venkatachalam, S., and Ko, S. B., Design of power and area efficient approximate multipliers. *IEEE Trans. VLSI Syst.* 25(5):1782–1786, 2017.
36. Gopeka, S. V., Murali, L., and Manigandan, T., VLSI Design of ECG QRS Complex Detection using Multiscale Mathematical Morphology, ICACCCT-14, 478–82, 2014.
37. Chen, S.-W., Chen, H.-C., and Chan, H.-L., A real-time QRS detection method based on moving-averaging incorporating with wavelet denoising. *Comput. Methods Programs Biomed.* 82(3): 187–195, 2006.
38. Poli, R., Cagnoni, S., and Valli, G., Genetic design of optimum linear and nonlinear QRS detectors. *IEEE Trans. Biomed. Eng.* 42(11):1137–1141, 1995.
39. Afonso, V. X., Tompkins, W. J., Nguyen, T. Q., and Luo, S., ECG beat detection using filter banks. *IEEE Trans. Biomed. Eng.* 46(2): 192–202, 1999.
40. Jeong, C.-I., Mak, P.-I., Lam, C.-P., Dong, C., Vai, M.-I., Mak, P.-U., Pun, S.-H., Wan, F., and Martins, R. P., A 0.83-uW QRS detection processor using quadratic spline wavelet transform for wireless ECG acquisition in 0.35-uM CMOS. *IEEE Trans. Biomed. Circuits Syst.* 6(6):586–595, 2012.